

INFLUENCE OF PORCELAIN TILE THICKNESS ON THE STRENGTH OF RAISED FLOOR SYSTEMS

Djeisa Pasini ^{1,2}, Angela Waterkemper Vieira ^{1,2}, Aline Demarch ^{1,2}, Laura Savi Rosso ^{1,2}, Sérgio Ruzza ², Elídio Angioletto ¹, Elaine G. P. Antunes ¹, Adriano Michael Bernardin ¹

¹ Graduation Program in Materials Science and Engineering, PPGCEM, University of the Extreme South of Santa Catarina, UNESC, Criciúma, 88806-000, Santa Catarina, Brazil

² Eliane Ceramic Tiles, Cocal do Sul, 88845-000, Santa Catarina, Brazil

ABSTRACT

Raised floor systems are mainly used in commercial environments and several materials are used as coverings, such as porcelain tiles. Consequently, the thickness of the tiles can influence the performance of raised floor systems and restrict their use. There are no studies on the use of ceramic tiles in raised floor systems regarding the supported loads and deformations. In this work, the effect of the thickness of a porcelain tile on the strength of raised floor system is studied, considering the stresses and strains as a function of the applied load. The breaking load, flexural strength, water absorption, and coefficient of restitution of a porcelain tile were determined according to ISO 10545 and ISO 13006 standards. The hard-body, soft-body and concentrated load impact resistance of the raised floor system was determined according to BS 7976 standard. ANOVA was used to analyze the maximum stress and strain supported by the system, as well as the coefficient of restitution and the impact damping factor. A qualitative analysis of the system was also carried out after the end of the tests. This showed that the layout of the bases had no influence on the strength of the raised floor system (p -value = 0.84; $R^2 = 91.3\%$).

On the other hand, the thickness of the ceramic tiles was critical for the maximum load withstood by the system (95% confidence level; p -value = 0.011; R^2 = 91.3%). As the thickness of the porcelain tile increased, system strength rose. The tensile strength of the raised floor system is related to the strength of the individual ceramic tiles. The average breaking load changed depending on tile thicknesses: for tiles with 12-mm thickness, the average breaking load was 3760 N; for tiles with 16-mm thickness, the average breaking load was 7041 N; and for tiles with 20-mm thickness, the average breaking load was 12268 N. Therefore, the thickness of the porcelain tiles changes the strength of a raised floor system. It is necessary to create a specific international standard for raised floor systems using ceramic materials to guide the proper selection of materials, ensuring the safety and performance of raised floor systems worldwide.

1. INTRODUCTION

The first applications of the raised floor system date back to the 1950s. However, since the 2000s the adoption of this system has been significant, driven by the advancement of the technology [1]. Since that time, this system has been used in corporate environments, mainly due to the efficiency of ventilation, air quality and reduction of energy consumption. In addition, the system can easily be installed in spaces under the cladding, providing ease of maintenance, giving users flexibility in changing the layouts of areas when necessary [2]. As a result, raised floor systems have been increasingly used, mainly in commercial buildings, often combined with "Underfloor Air Distribution" (UFAD), a system for air distribution in open areas under the raised floor. This integration provides buildings with better air circulation, increasing energy efficiency and air quality [3].

Because communications are processed using computers and the technologies are based on the Internet, companies have had to adapt to them [4]. These systems correspond to 50% of new construction projects in Germany, Austria, and Denmark, according to Olesen [5]. They are installed in 85% of rural homes in northern China, according to Zhuang et al. [6] and in almost all residential buildings in Korea [7]. These numbers have increased significantly over time worldwide.

Therefore, the development of products and structures used for raised floor systems has also undergone many innovations. Modern raised floor systems can feature a variety of floor panels, understructures, and auxiliary components [8]. The system can be composed of different types of materials and has complex layers and geometries and must meet structural performance requirements [9].

The raised floor systems presented in this work consist of self-locking removable floor plates, supported on telescopic supports, both made of thermoplastic polypropylene, which establish a space between the concrete base and the finished raised floor [10]. The finishing layer of the system can be formed by various materials, such as concrete, carpet, natural rock slabs, wood, and ceramics, especially porcelain tiles, or even new materials such as phase-change materials (PCMs) [11].

Regarding porcelain tiles, according to CSTB [12], the minimum thickness must be 18 mm; however, the current European market usually uses a thickness of 20 mm.

Ceramic materials have a limited capacity for plastic deformation in most of their applications, presenting a brittle behavior. Therefore, the mechanical resistance of these materials is dictated by the material's ability to undergo the application of a load without failing by rupture, and ceramics are particularly sensitive to the presence of internal flaws, which determine their ultimate strength [13].

As ceramic tiles are frequently used in raised floor systems, it is necessary to consider the intrinsic properties that directly influence their performance. Although there are studies focused on the thermal performance of raised floor systems [14][15][16][17][18][19][20][21], there are no works evaluating the loads and deformations of raised floor systems when using porcelain tiles as the finishing layer.

Therefore, this work was undertaken to analyze the loads and deformations of raised floor systems when porcelain tile is used as covering/finishing layer. An unglazed porcelain tile was used with 12-, 16- and 20-mm thicknesses.

2. MATERIALS AND METHODS

The first step was the selection of the elements of the raised floor system. A polypropylene base and an unglazed porcelain tile were used. The height of the system was adjusted to 1200 mm using a rigid tube, the most critical height according to the manufacturer's specifications. The unglazed porcelain samples were classified as BIa UGL, measuring 60×60 cm, with thicknesses of 12, 16 and 20 mm. The thicknesses were measured according to ISO 10545 [22][23] and the breaking load, flexural strength modulus and water absorption were determined according to the same standard. The raised floor systems were built to carry out the hard body, soft body, and concentrated load impact tests, all in triplicate for each thickness.

In the hard body and soft body impact tests, the main factor was the region of impact on the porcelain tile surface, located in the center of the systems (sets) for both tests, according to the BS EN 12825 standard. For the hard body test, the masses of the impact bodies were reduced from 4.5 kg to 250, 350 and 500 g to avoid perforating the tiles and thus obtain the restitution coefficients. The coefficients were determined using an accelerometer (PCB Piezotronics 350C04) fixed to the surface of the ceramic tile. The data was analyzed by LabView® software using a signal conditioner.

In the concentrated load test, deformations were measured at pre-defined load application positions. Strain gauges were positioned on the surface of the ceramic tiles and vertical displacements were measured using an LVDT, both connected to a data acquisition unit, controlled by the Catman Easy software.

The contact area of the load applicator and the position of the strain gauges (A, B and C) were determined according to the standard guidelines for the center of the raised system, the center of an edge, on the side of the raised system, and the most fragile area of the system. To identify a potentially more fragile area, the set of supports (bases) of the raised floor system was examined, Fig.1. The areas marked in green correspond to the regions where the supports connect to the system and, therefore, the region devoid of support points (bases) was identified as the most vulnerable. This illustration offers a detailed view of the load configuration in relation to the system's support points.

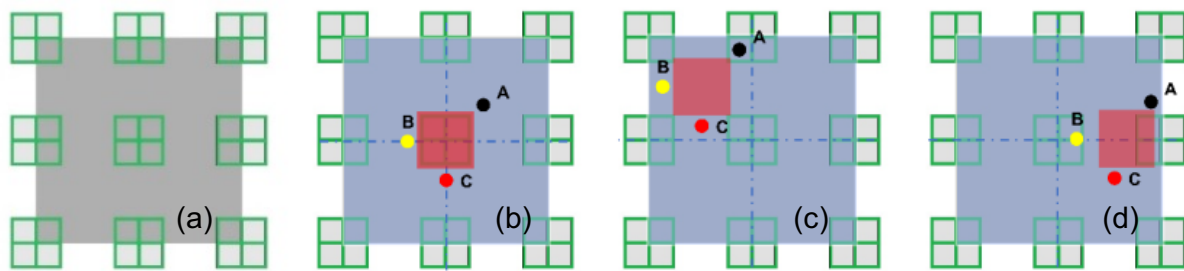


Figure 1. Concentrated load test according to BS EN 12825 standard: (a) Top view of the base coupling; (b) Set 1; (c) Set 2; (d) Set 3

Set 01, placed in the center of the raised system, covers the entire area of a support, positioned directly below the region where the load is applied. Set 3 covers half the area of a support, while for set 2 there is no support under the area where the load is applied in the raised systems.

A 2^k factorial experimental design was used with three central points, where the thickness of the tiles and the position where the load is applied are the main factors. The strength of the raised floor systems is the response. The factors and levels were determined based on the concentrated load test variables according to the BS EN 12825 standard (2001).

The thicknesses were defined based on the tiles commonly used in raised floor systems, both in Brazil and Europe. Level (0) corresponds to the thickness usually used in raised floor systems in the Brazilian market. Level (-1) was defined to reduce costs for a lower thickness. Level (+1) was defined based on the thickness commonly used in raised floor systems in the European market. The sets, which define the position where the load was applied on the raised systems, were defined according to regulatory guidelines. Level (-1) was established as the center of the system, level (+1) at the center of one of the edges, and level (0) between these two positions.

3. RESULTS AND DISCUSSIONS

a) Breaking load and flexural strength modulus:

The breaking load and flexural strength modulus for the porcelain tile used in the study can be seen in Fig.2. The blue bars represent the breaking load while the red line shows the flexural strength. The samples showed breaking loads and flexural strengths in accordance with those specified by the ISO 13006 [24] standard, exceeding the minimum values of 1500 N and 35 MPa, respectively.

As tile thickness increases, the breaking load increases. All samples have the same modulus of rupture, regardless of the thickness. According to Silva et al. [25], breaking load is linked to the microstructure of the material. For a constant microstructure, a thicker tile will have a higher breaking load compared to thinner tiles. Flexural strength is also related to a material's microstructure, so samples with different thicknesses and the same microstructural composition tend to have a similar modulus. The same breaking load behavior with regard to thickness was found by Abad-Coronel et al. [26].

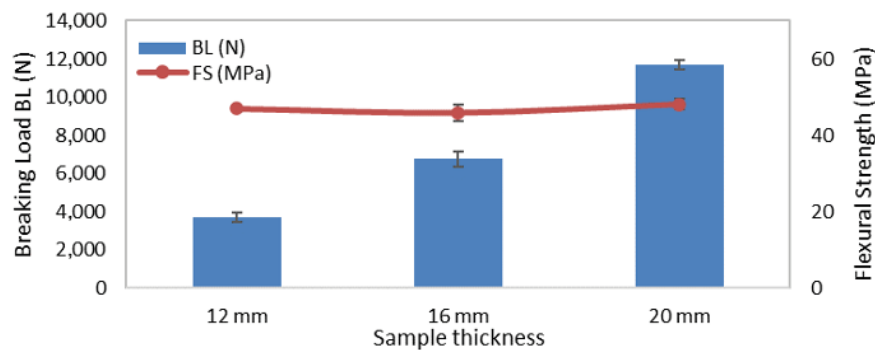


Figure 2. Breaking load (BL) and flexural strength (FS) (MPa) of the porcelain tiles

b) Water absorption and apparent density

The water absorption (WA) of the samples is shown in Fig.3. The blue bars show the water absorption, and the red lines show the apparent density. The water absorption of the tiles was below 0.1 wt.%, being classified as BIa UGL, according to the ISO 13006 [24] standard for porcelain tiles. There is a slight tendency for water absorption to increase with reduced thickness. The thinner samples were prepared by machining the surface of the tiles, therefore opening the pores near the surface, increasing the open porosity and the water absorption. Wiśniewska et al. [27] showed that increasing the open porosity also increases water absorption. All samples showed similar apparent density and flexural strength [28]. García-Ten et al. [29] show a linear relationship between the flexural strength and the apparent density of the material ($R^2 = 0.997$).

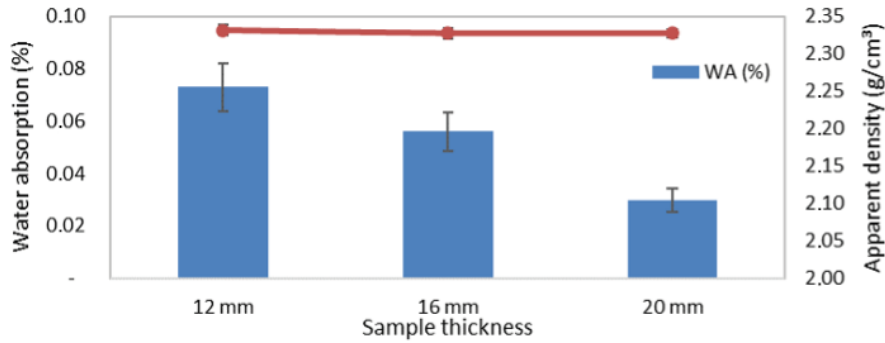


Figure 03. Water absorption (%) and apparent density (g/cm³)

c) Hard body impact:

The average coefficient of restitution (KR, dimensionless) of the raised systems subjected to the hard body impact is shown in Tab.1 for the mass of the impact bodies (250, 350 and 500 g) and thicknesses of the tiles (20, 16 and 12 mm).

Height (m)	Energy (J)	Mass (g)	DBS1 12	DBS1 16	DBS1 20
0.6	1.5	250	0.11	0.20	0.32
0.6	2.1	350	Failure	Failure	0.25
0.6	3.0	500	Failure	Failure	0.14

Table 1. Analysis of the coefficient of restitution (KR) in the hard body impact test

The tests performed with the 500 g body resulted in failure of the 12- and 16-mm raised systems at the first impact, and the restitution coefficient was not determined for them. For the 20-mm raised system, failure occurred at the third impact, and the average KR was 0.14. Regardless of the thickness, no raised system complied with the standard specifications. For the 350 g impact body, the 12- and 16-mm raised systems failed at the first impact. The 20-mm system resisted the impact of three impacts without failure, resulting in an average KR = 0.25. All systems resisted the impacts of the 250 g body. The 12-, 16- and 20-mm prototypes resisted three consecutive impacts without failure. The average KR values were 0.11, 0.20 and 0.32, respectively. The failures due to the hard body impact tests are shown in Fig.4.

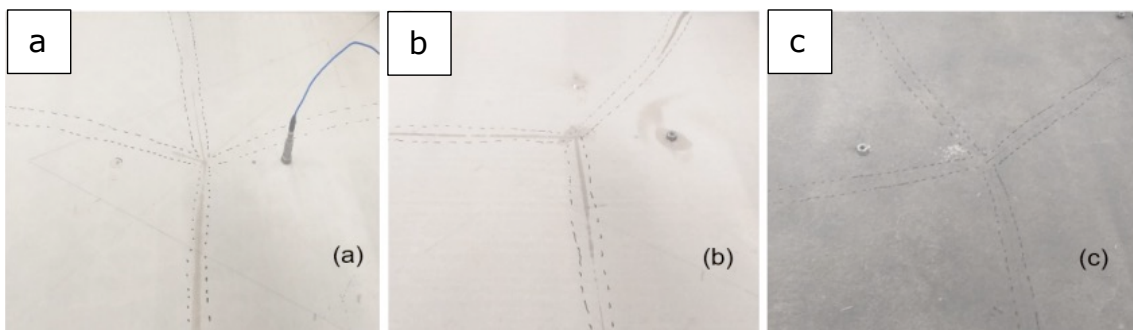


Figure 4. Hard body impact test (a) DBS1 12 (b) DBS1 16 (c) DBS1 20

d) Soft body impact:

The analysis of the soft body impact test was divided into the raised floor system (polypropylene material) and the porcelain tile (ceramic material) for the worst failure of the raised systems. The soft body impact test of the raised floor systems is shown in Tab.2 considering the height of the impact body release (0.30-2.40 m) for the 12-, 16- and 20-mm systems (MBS1 12, MBS1 16 and MBS1 20, respectively). The failed tiles and collapsed system (marked with * in Tab.2) after impact are shown in Fig.5.

Altura (m)	Energía (J)	MBS1 20	MBS1 16	MBS1 12
0.30	120	No failure	No failure	Tile failed*; system collapsed
0.45	180	No failure	No failure	-
0.60	240	No failure	No failure	-
0.90	360	No failure	Tile failed*; system failed	-
1.00	400	No failure	-	-
1.20	480	No failure	-	-
1.80	720	Tile, no failure; system collapsed*	-	-
2.40	960	-	-	-

Table 2. Qualitative analysis of the soft body impact test

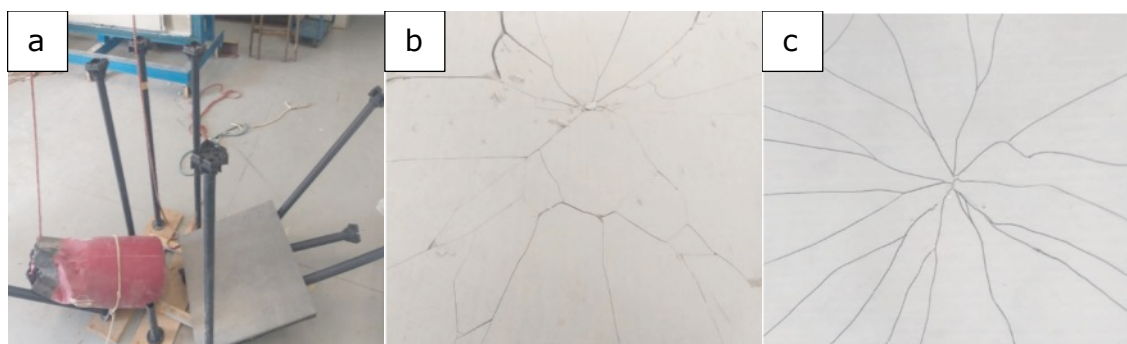


Figure 5. Soft body impact test (a) MBS1 20 system collapse; (b) MBS1 16 porcelain tile failure (360 J); (c) MBS1 12 porcelain tile failure (120 J)

The 20-mm raised floor system (MBS1 20) collapsed with an impact energy of 720 J; the porcelain tiles did not fail. Therefore, the support had lower performance than the porcelain tiles. The support and the porcelain tiles showed the same performance for the 16-mm system (MBS1 16), failing at an energy of 360 J. For the 12-mm raised floor system, the support performed better than the porcelain tiles, as the tiles failed with an impact energy of 120 J and the supports remained intact.

According to the BS EN 12825 (2001) standard, the raised system should not collapse under an impact energy of 400 J (corresponding to a soft body impact at 1 m height). Therefore, in this work, only the MBS1 20 prototype, with a tile thickness of 20 mm, passed the test.

e) Concentrated load (BS EN 12825)

For the concentrated load test, load (N) versus deformation (μm) was determined considering the tile thicknesses and raised floor systems, Fig.6. The load was applied to the raised systems until any component failed.

For all sets, the 20-mm raised floor system showed the highest resistance, followed by the 16-mm system and finally the 12-mm system. Therefore, the failure resistance of the raised floor system depends on the thickness of the ceramic tile, that is, the greater the tile thickness, the greater the mechanical resistance of the raised floor system [30][31], mainly when the microstructure of the tiles is the same independently of the thickness [25].

Regarding deformation, ceramic materials show limited elastic deformation, as they have a higher modulus of elasticity, low plastic deformation and, therefore, greater flexural rigidity, that is, they are brittle materials [32]. However, as the raised floor system is a set of polymeric and ceramic materials, the deformation was influenced by the polymeric material with an elastic behavior as opposed to that of the ceramic material [33]. The deformation of sets 1 and 3 (see Fig.1) was higher for 12-, 16- and 20-mm porcelain tile thicknesses, in this order. For set 2, the 12- and 16-mm systems showed similar deformation. The 20-mm system showed the smallest deformation, and the polypropylene support broke before the ceramic tile.

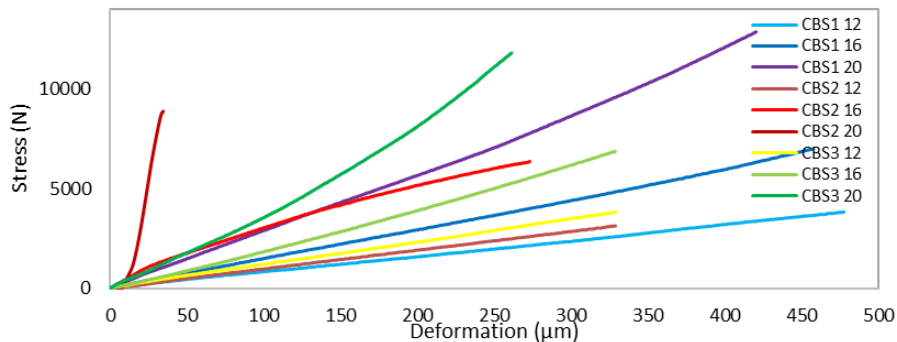


Figure 6. Concentrated load test according to BS EN 12825; stress \times strain curve

Lamnini et al. [34] studied the stress-strain curves for ceramic and composite materials, showing similar elastic behavior. However, in this work, the stress-strain curves show the elastic behavior of the ceramic tiles + polypropylene support of the raised floor systems, and the elastic behavior is different.

The load versus raised system sets (load positions) are shown in Fig.7. The blue bars show the maximum load supported by the systems. The set configurations and failure types are shown on the horizontal axis. Failures in the porcelain tiles are indicated as "PP", while the collapse in the system support are identified as "SPE". The error bars comprise the standard deviation for three samples.

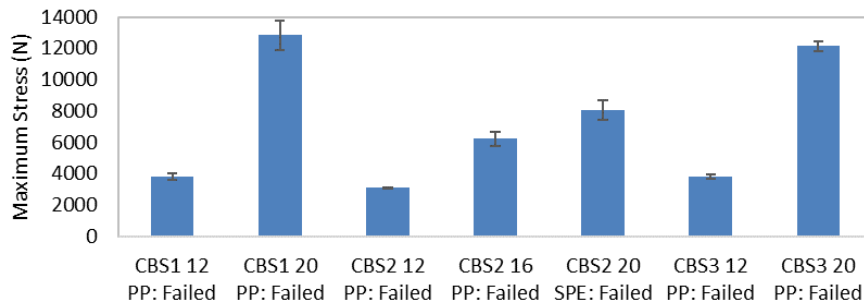


Figure 7. Concentrated load test according to BS EN 12825; maximum load × sets

Sets 1 and 3 show the highest resistance to failure for the same thickness (12 and 20 mm) due to the higher maximum loads for these loading positions (see the error bars). For set 1, the load is applied directly on the whole area of the PP support. The load is applied over half of the area of the PP support on set 3. On set 2, there is no supporting component under the load, and this set is the most fragile raised system (see Fig.1). The CBS2 20 raised system (set 2, 20-mm tile) shows a distinct behavior. There was a collapse in the PP support before the failure of the porcelain tile, which remained intact, Fig.8.

The buckling behavior of the polypropylene support of the raised floor system is also an important factor for analysis. Ostrowski et al. [35] and Sun et al. [36] analyzed buckling under axial compression of metallic alloy tubes and the visual analysis of buckling of this work. However, the stress-strain curves are totally different. On the other hand, for CBS1 20 and CBS3 20 systems (sets 1 and 3, respectively, for 20-mm tiles) only bending of the tiles occurred.

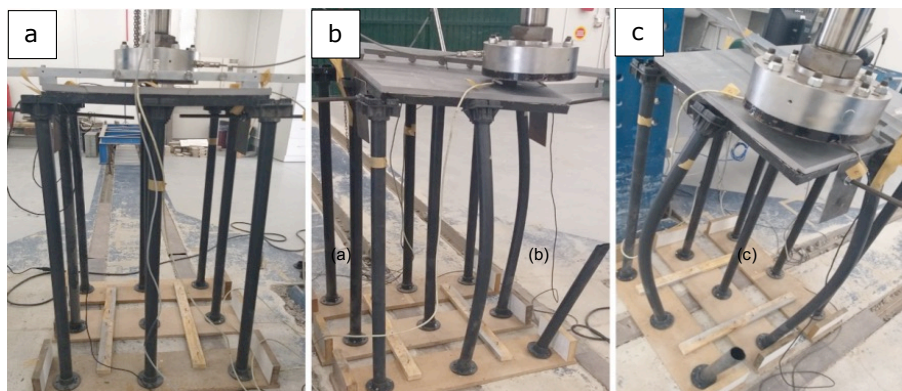


Figure 8. Concentrated load test according to BS EN 12825: (a) DBS1 20; (b) DBS2 20 front side; (c) DBS2 20 lateral side

The BS EN 12825 (2001) standard establishes that raised floor systems must have a minimum breaking load (L) equal to or greater than 4000 N and a maximum vertical displacement of 4 mm. However, the raised floor system with 12-mm thick porcelain tiles did not meet this standard, as their breaking load was below 4000 N. On the other hand, the 16- and 20-mm raised systems met the requirements.

Regarding deformation, the vertical displacements in each system were less than 2.5 mm, and all systems complied. Therefore, the CBS 16 system was classified as 2A and the CBS 20 system as 5A, according to the standard.

The breaking load of the raised floor systems and that of the porcelain tiles alone can be seen in Fig.9. The blue bars show the maximum breaking load of the porcelain tiles, and the red bars show the maximum breaking load of the complete raised floor systems. The error bars comprise the standard deviation.

Considering the standard deviations, the polymeric supports do not increase the strength of the raised system regarding the strength (breaking load) of the porcelain tiles. Therefore, the strength of the raised floor system as a whole is equal to the strength of the ceramic tiles ($R^2 = 0.999$ by Pearson's correlation coefficient).

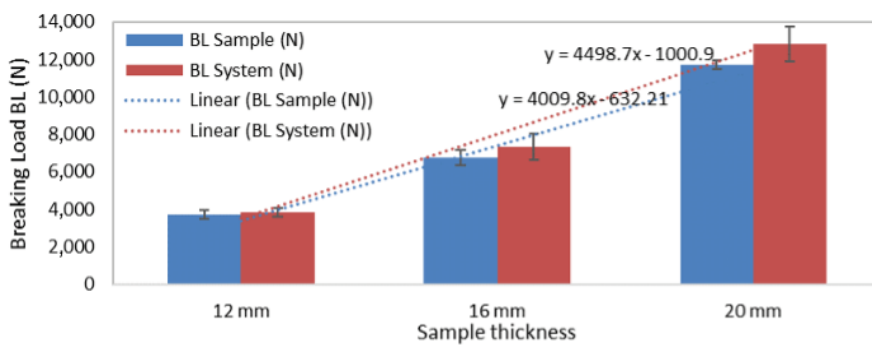


Figure 9. Correlation of the breaking load of ceramic tiles and the breaking load of the raised floor system

The linear regression for the ceramic tile is $y = 4009.8x - 632.21$ and that of the raised floor system is $y = 4498.7x - 1004.9$. Therefore, breaking load is influenced by tile thickness. The greater the thickness, the greater the breaking load, and the expected breaking load for a different thickness can be determined. As a result, it is possible to evaluate the expected performance of the ceramic tile at different thicknesses, making the appropriate specification for the desired application, ensuring that the chosen thickness meets the necessary resistance requirements.

5. CONCLUSIONS

The analysis of the raised floor systems showed that the thickness of the porcelain tile directly affects the resistance of the system. The increase in the thickness of the tiles provided an increase in the load supported by the system, making the porcelain tiles suitable for use in the raised floor system. The configuration of the supports is enough to guarantee an even resistance of the system, that is, the loading position has little impact on the maximum load supported by the system.

The raised floor systems of this work do not meet all the requirements of the BS EN 12825 (2001) standard. In the hard body impact test, all systems failed. In the soft body impact test, only the raised system with 20-mm thick porcelain tiles complied. Regarding the concentrated load test, only the 16- and 20-mm thick porcelain tiles complied. However, the requirements of this standard may not be the most appropriate to limit the application of ceramic materials in these systems.

The present work not only helped to determining that the adequate thickness of porcelain tiles specified for use in raised floor systems will depend on the location where the system will be installed, but also as an indicator of the need to create a standard specific for raised floor systems using ceramic materials.

6. REFERENCES

- [1] Lin YJP, Linden PF, 2005. A model for an underfloor air distribution system. *Energy and Buildings* 37, 4, 399-409. <http://dx.doi.org/10.1016/j.enbuild.2004.07.011>
- [2] Schiavon S, Lee KH, Bauman F, Webster T, 2010. Influence of raised floor on zone design cooling load in commercial buildings. *Energy and Buildings* 42, 8, 1182-1191. <http://dx.doi.org/10.1016/j.enbuild.2010.02.009>
- [3] Ahmad S, Goga G, Mohan R, 2023. Predicting the thermal comfort of occupants in an indoor auditorium space with different UFAD ventilation arrangements. *Materials Today Proceedings* 80, 62-69. <http://dx.doi.org/10.1016/j.matpr.2022.10.115>
- [4] Pasut W, Bauman F, Carli M, 2014. The use of ducts to improve the control of supply air temperature rise in UFAD systems: CFD and lab study. *Applied Energy* 134, 490-498. <http://dx.doi.org/10.1016/j.apenergy.2014.08.002>
- [5] Olesen BW, 2002. Radiant floor heating in theory and practice. *ASHRAE Journal* 44, 19.
- [6] Zhuang Z, Li Y, Chen B, Guo J, 2009. Chinese kang as a domestic heating system in rural northern China. A review. *Energy and Buildings* 41, 1, 111-119. <http://dx.doi.org/10.1016/j.enbuild.2008.07.013>
- [7] Yeo M-S, Yang I-H, Kim K-W, 2003. Historical changes and recent energy saving potential of residential heating in Korea. *Energy and Buildings* 35, 7, 715-727. [http://dx.doi.org/10.1016/s0378-7788\(02\)00221-9](http://dx.doi.org/10.1016/s0378-7788(02)00221-9)
- [8] Zhang G, Yang J, Sidwell A, 2002. Raised floor system: a paradigm of future office building fitout? *Advances in Building Technology* 1577-1584. <http://doi.org/10.1016/B978-008044100-9/50195-9>
- [9] Kim D-W, Joe G-S, Park S-H, Yeo M-S, Kim K-W, 2017. Experimental evaluation of the thermal performance of raised floor integrated radiant heating panels. *Energies* 10, 10, 1632. <http://dx.doi.org/10.3390/en10101632>
- [10] Idalêncio GF et al, 2022. Raised floor systems with ceramic tiles. *Journal of Engineering* 8, 6, 13-27. http://dx.doi.org/10.24840/2183-6493_008.006_0002
- [11] Kitagawa H, Asawa T, Rio MA, Kubota T, Trihamdani AR, 2023. Thermal energy simulation of PCM-based radiant floor cooling systems for naturally ventilated buildings in a hot and humid climate. *Building and Environment* 238, 110351. <http://dx.doi.org/10.1016/j.buildenv.2023.110351>
- [12] CSTB, 2018. Revêtements de sol céramiques. Spécifications techniques pour le classement. UPEC 92.
- [13] Xiao Z et al, 2020. Materials development and potential applications of transparent ceramics: a review. *Materials Science and Engineering R* 139, 100518. <http://dx.doi.org/10.1016/j.mser.2019.100518>
- [14] Bauman FS, 2003. Underfloor air distribution (UFAD) design guide. *ASHRAE Journal*.
- [15] Zhang K, Zhang X, Li S, Jin X, 2014. Review of underfloor air distribution technology. *Energy and Buildings* 85, 180-186. <http://dx.doi.org/10.1016/j.enbuild.2014.09.011>
- [16] Raftery P, Bauman F, Schiavon S, Epp T, 2015. Laboratory testing of a displacement ventilation diffuser for underfloor air distribution systems. *Energy and Buildings* 108, 82-91. <http://dx.doi.org/10.1016/j.enbuild.2015.09.005>
- [17] Gao Y, Liu J, Yuan X, Zhang K, Yang Y, Wang Y, 2017. Air-conditioning system with underfloor air distribution integrated solar chimney in data center. *Procedia Engineering* 205, 3420-3427. <http://dx.doi.org/10.1016/j.proeng.2017.09.852>
- [18] Yuan X, Xu X, Liu J, Pan Y, Kosonen R, Gao Y, 2020. Improvement in airflow and temperature distribution with an in-rack UFAD system at a high-density data center. *Building and Environment* 168, 106495. <http://dx.doi.org/10.1016/j.buildenv.2019.106495>
- [19] Fan Y, Li X, Zheng M, Weng R, Tu J, 2020. Numerical study on effects of air return height on performance of an underfloor air distribution system for heating and cooling. *Energies* 13, 5, 1070. <http://dx.doi.org/10.3390/en13051070>
- [20] [20] underfloor air distribution system. *Journal of Building Engineering* 57, 104800. <http://dx.doi.org/10.1016/j.jobbe.2022.104800>
- [21] Chen M, Zhang Z, Deng Q, Feng Y, Wang X, 2023. Optimization of underfloor air distribution systems for data centers based on orthogonal test method: a case study. *Building and Environment* 232, 110071. <http://dx.doi.org/10.1016/j.buildenv.2023.110071>
- [22] ISO 10545-2, 2018. Ceramic tiles. Part 2: Determination of dimensions and surface quality. Switzerland: International Standardization Organization.
- [23] ISO 10545-4, 2019. Ceramic tiles. Part 4: Determination of modulus of rupture and breaking strength. Switzerland: International Standardization Organization.
- [24] ISO 13006, 2018. Ceramic tiles. Definitions, classification, characteristics and marking Switzerland: International Standardization Organization.
- [25] Silva AL, Feltrin J, Bó MD, Bernardin AM, Hotza D, 2014. Effect of reduction of thickness on microstructure and properties of porcelain stoneware tiles. *Ceramics International* 40, 9, 14693-14699. <http://dx.doi.org/10.1016/j.ceramint.2014.05.150>
- [26] Abad-Coronel C, Paladines Á, Ulloa AL, Paltán CA, Fajardo JI, 2023. Comparative fracture resistance analysis of translucent monolithic zirconia dioxide milled in a CAD/CAM system. *Ceramics* 6, 2, 1179-1190. <http://dx.doi.org/10.3390/ceramics6020071>
- [27] Wiśniewska K, Pichór W, Kłosek-Wawrzyn E, 2021. Influence of firing temperature on phase composition and color properties of ceramic tile bodies. *Materials* 14, 21, 6380. <http://dx.doi.org/10.3390/ma14216380>
- [28] Darweesh HHM, 2019. Recycling of glass waste in ceramics. Part I: physical, mechanical and thermal properties. *SN Appl. Sci.* 1, 1274. <https://doi.org/10.1007/s42452-019-1304-8>
- [29] García-Ten J, Saburit A, Bernardo E, Colombo P, 2012. Development of lightweight porcelain stoneware tiles using foaming agents. *Journal of The European Ceramic Society* 32, 4, 745-752. <http://dx.doi.org/10.1016/j.jeurceramsoc.2011.10.028>

- [30] Farzad M, Shafieifar M, Azizinamini A, 2019. Experimental and numerical study on an innovative sandwich system utilizing UPFRC in bridge applications. *Engineering Structures* 180, 49-356. <http://dx.doi.org/10.1016/j.engstruct.2018.11.052>
- [31] Wang W, Sun K, Liu H, 2020. Effects of different aluminum sources on morphologies and properties of ceramic floor tiles from red mud. *Construction and Building Materials* 241, 118119. <http://dx.doi.org/10.1016/j.conbuildmat.2020.118119>
- [32] Collini L, Carfagni GR, 2014. Flexural strength of glass-ceramic for structural applications. *Journal of The European Ceramic Society* 34, 11, 2675-2685. <http://dx.doi.org/10.1016/j.jeurceramsoc.2013.10.032>
- [33] Chawla KK, 2019. *Composite Materials*. Springer International Publishing. <http://dx.doi.org/10.1007/978-3-030-28983-6>
- [34] Lamnini S, Pugliese D, Bairo F, 2023. Zirconia-based ceramics reinforced by carbon nanotubes: a review with emphasis on mechanical properties. *Ceramics* 6, 3, 1705-1734. <http://dx.doi.org/10.3390/ceramics6030105>
- [35] Ostrowski K, Dudek M, Sadowski Ł, 2020. Compressive behaviour of concrete-filled carbon fiber-reinforced polymer steel composite tube columns made of high-performance concrete. *Composite Structures* 234, 111668. <http://dx.doi.org/10.1016/j.compstruct.2019.111668>
- [36] Sun Z-C, Cao J, Huang L, Yin Z-K, Zheng L-S, 2021. Buckling behavior of AA6061 circular tube under axial compression by considering contact condition of tube end. *International Journal of Lightweight Materials and Manufacture* 4, 3, 383-392. <http://dx.doi.org/10.1016/j.ijlmm.2021.06.001>